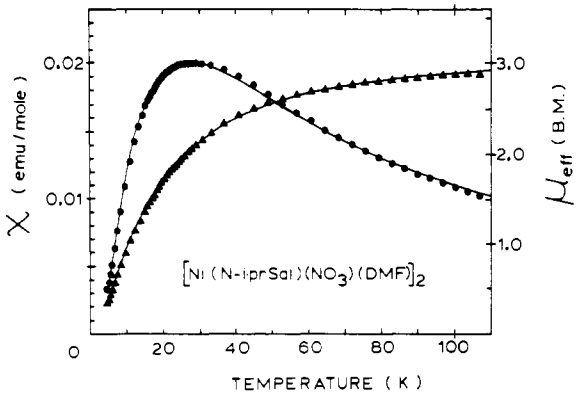


**Figure 9.** Plots of the magnetic susceptibility and effective magnetic moment of $[Ni(ips)(NO_3)DMF]_2$ as a function of temperature. The complex has "trans" structure **3** and is an antiferromagnetic dimer (type c).

**Table IV.** Parameters for the Fit of the Magnetic Data to the $\chi(g,J,D,zJ')$ Equation for $[Ni(R\text{-}sal)(NO_3)R']_2$

| | R′ = 2-pic R = phenyl | R′ = EtOH R = isopropyl | R′ = DMF R = isopropyl |
|---|---|---|---|
| | i. $zJ' = 0$ | | |
| $g$ | 2.12 ± 0.02 | 2.19 ± 0.01 | 2.32 ± 0.01 |
| $J/k$, K | 13.0 ± 0.2 | 19.0 ± 0.5 | −13.3 ± 0.1 |
| ($J$, cm$^{-1}$) | (9.0) | (13.2) | (−9.2) |
| $D/k$, K | 7.9 ± 0.2 | 9.2 ± 0.5 | 17.0 ± 1.0 |
| ($D$, cm$^{-1}$) | (5.5) | (6.4) | (11.8) |
| | ii. $zJ' \neq 0$ | | |
| $g$ | 2.12 ± 0.02 | 2.15 ± 0.02 | 2.31 ± 0.02 |
| $J/k$, K | 12.5 ± 1.0 | 23.0 ± 1.0 | −13.3 ± 0.05 |
| ($J$, cm$^{-1}$) | (8.7) | (16.0) | (−9.2) |
| $D/k$, K | 19.2 ± 1.0 | 22.0 ± 1.0 | 16.0 ± 1.0 |
| ($D$, cm$^{-1}$) | (13.3) | (15.3) | (11.1) |
| $zJ'/k$, K | 0.1 ± 0.1 | 0.3 ± 0.1 | 0.5 ± 0.1 |
| ($J'$, cm$^{-1}$) | (0.07) | (0.14) | (0.3) |

dicular to the $Ni_2O$ bridging plane.

The major difference in the pathway of spin exchange is in the orientation of the electron orbitals on the bridging oxygens. In all three cases the Ni–O(1)–C(2) bonding angle is reasonably close to 120°. This angle indicates that oxygen is $sp^2$ hybridized with the $p_z$ orbital probably involved in $\pi$ overlap with the aromatic ring. In the antiferromagnetic case, all nickel–oxygen bridging $\sigma$ bonds involve $sp^2$ hybrid orbitals on the oxygen and the $d_{x^2-y^2}$ orbital on the nickel. In addition there may also be a significant $\pi$ overlap between the nickel $d_{z^2}$ orbitals and the oxygen $p_z$ orbital. In the ferromagnetic case, one nickel–oxygen $\sigma$ bond uses an $sp^2$ oxygen orbital and the other nickel–oxygen $\sigma$ bond uses a $p_z$ oxygen orbital. There is no $\pi$ overlap possible between the two nickel(II) centers for this case.

The electron orbital overlap integral for the magnetic exchange may be expressed as a combination of $\sigma$ and $\pi$ contributions having the form $\langle (Ni)3d_{x^2-y^2}\|(O)sp^2\|(Ni')3d_{x^2-y^2}\rangle$ and $\langle (Ni)3d_{xz}\|(O)p_z\|(Ni')3d_{z^2}\rangle$ for the antiferromagnetic case, and the $\sigma$-bonding pathway $\langle (Ni)3d_{x^2-y^2}\|(O)sp^2\perp(O)p_z|(Ni)3d_{z^2}\rangle$ for the ferromagnetic case. The notation for these electron orbital overlap expressions is defined elsewhere.[15,16] The symbols | and $\perp$ represent magnetically compatible and magnetically orthogonal overlap, respectively.

The magnetic orthogonality principle of the orbital symmetry relationships has been used to predict the sign and magnitude of the magnetic exchange.[15,16] The presence of magnetic orthogonality in the overlap integral ($\perp$) is one of the conditions that will permit ferromagnetic exchange. The observed exchange pathways obtained from the crystal structures and the complementary magnetic data are easily correlated with the symmetry relationships of the bridging orbitals on the phenolic oxygen.

In the case where one Ni–O bridging bond involves a $p_z$ oxygen orbital (cis, cases a and b), the expected ferromagnetic interaction is observed. On the other hand, the effectiveness of the $\sigma$, $\pi$ overlap integral in propagating antiferromagnetic exchange is evident from the observed strong antiferromagnetic coupling of the two nickel(II) centers.

**Acknowledgment.** Support under NSF Grant CHE77-01372, and from the Research Corp., is gratefully acknowledged.

**Registry No.** $[Ni(ps)(NO_3)(2\text{-pic})]_2\cdot 2CH_2Cl_2$, 78199-16-3; $Ni_2(ips)_2(NO_3)_2(EtOH)_2$, 78199-17-4; $[Ni(ips)(NO_3)DMF]_2$, 78199-18-5; $Ni(ps)_2$, 38929-70-3; $Ni(ips)_2$, 41754-10-3.

**Supplementary Material Available:** Tables of magnetic susceptibilities, analytical data, and observed and calculated structure factors (30 pages). Ordering information is given on any current masthead page.

(15) Ginsberg, A. P. *Inorg. Chim. Acta, Rev.* **1971**, *5*, 45.
(16) Anderson, P. W. *Magnetism* **1963**, *1*.

Contribution from the Department of Chemistry, University of Maine, Orono, Maine 04469

# Laser-Excited Luminescence and Absorption Study of Monomer and Cluster Tetracyanopalladate(II) Species in Mixed Crystals

A. KASI VISWANATH, JEANETTE VETUSKEY, WILLIAM D. ELLENSON, MARY BETH KROGH-JESPERSEN, and HOWARD H. PATTERSON*

*Received January 13, 1981*

Laser-excited luminescence studies of $Pd(CN)_4^{2-}$ ions doped in NaCl crystals have demonstrated the existence of $Pd(CN)_4^{2-}$ clusters with the luminescence similar to that from single crystals of $BaPd(CN)_4\cdot 4H_2O$. Also, for mixed crystals of NaCN and KCN, luminescence from $Pd(CN)_4^{2-}$ clusters was observed. The optical absorption and MCD spectra of monomer species in palladium-doped crystals of alkali halides were assigned on the basis of MO calculations. The separation of the $a_{2u}$ and $e_u$ electronic states for $Pd(CN)_4^{2-}$ in alkali halides was found to be greater than that for $Pd(CN)_4^{2-}$ in solution.

## Introduction

The tetracyanide compounds of Ni, Pd, and Pt in the solid state form polymer chains with metal–metal bonding and show unusual properties which are not found in their aqueous solutions.[1-10] The best example among the tetracyanides is $K_2Pt(CN)_4Br_{0.3}\cdot 3H_2O$ (KCP) which has a large electrical conductivity at room temperature.[3] There are no palladium

(1) J. S. Miller and A. J. Epstein, *Prog. Inorg. Chem.*, 20 (1976).
(2) K. Krogmann, *Angew. Chem., Int. Ed Engl.*, **8**, 38 (1969).

0020-1669/81/1320-3493$01.25/0 

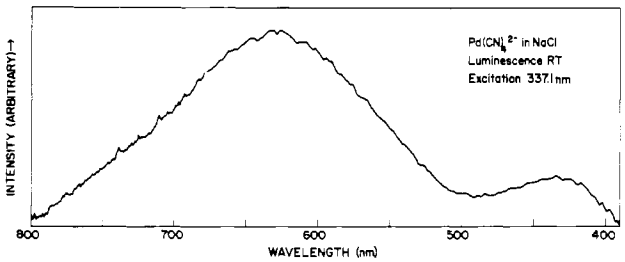


**Figure 1.** Laser-excited luminescence spectrum at room temperature for a single crystal of NaCl doped with $Pd(CN)_4^{2-}$ ions. Excitation wavelength is 337.1 nm.

compounds known in the literature which are similar to KCP. It is interesting to compare the optical properties of $Pd(CN)_4^{2-}$ with those of $Pt(CN)_4^{2-}$ to understand the differences in their electronic structure.[11,12]

We have recently studied the optical properties of interacting tetracyanoplatinate(II) ions in frozen aqueous solutions, pellets, pure single crystals, and mixed crystals of alkali halides and alkali cyanides.[13] In alkali halides, $Pt(CN)_4^{2-}$ ions exist as monomer, dimer, and cluster-type units, while in KCN crystals the $Pt(CN)_4^{2-}$ ions exist as polymer chains ($n = \infty$) or clusters ($n \geq 3$). Also, we have reported the laser-excited emission from $BaPd(CN)_4 \cdot 4H_2O$ pure single crystals.[14] In this paper we will discuss the optical spectra of $Pd(CN)_4^{2-}$ ions in mixed crystals of alkali halides and alkali cyanides, pellets, and aqueous solutions.

## Experimental Section

Mixed crystals of NaCl and KCl doped with $Pd(CN)_4^{2-}$ have been grown by slow evaporation of the respective saturated aqueous solutions to which a small amount of impurity ions has been added. Sodium cyanide and potassium cyanide crystals doped with $Pd(CN)_4^{2-}$ have been grown by the Bridgman method.

For the luminescence measurements, a Molectron Corp. UV 14 pulsed-nitrogen laser was used to excite the samples. The excitation wavelength of the $N_2$ laser is 337.1 nm. For selective excitation wavelength experiments, we used a Molectron Corp. DL-II Series Tunable Dye Laser pumped by the nitrogen laser. High-energy excitation in the UV region was accomplished with a KDP crystal as the frequency doubler. The luminescence was detected with a McPherson Model 2051 monochromator coupled to a PAR Model 124A lock-in amplifier and phootomultiplier. However, the lifetime measurements and time-resolved experiments were carried out with a Model 162 PAR boxcar integrator. The minimum lifetime that can be measured with our setup is ~10 ns.

The optical absorption spectra were recorded with a Cary 17D spectrophotometer. The low-temperature measurements in the range of 4–300 K were carried out with an Air Products LT-3-110 liquid-helium transfer Heli-Tran. Magnetic circular dichrosim experiments have been done with a Cary Model CD 60 instrument and a 60-kG superconducting magnet.

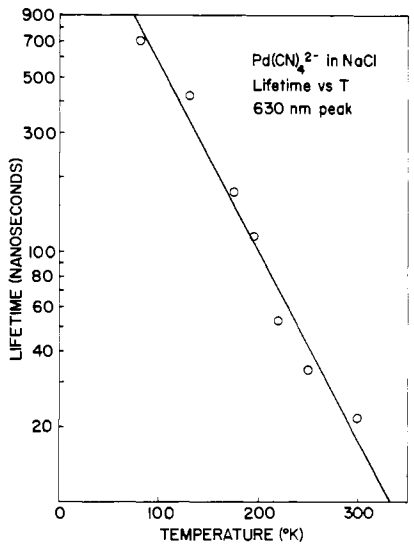


**Figure 2.** Variation of lifetime as a function of temperature for the 6300-Å band in a NaCl crystal doped with $Pd(CN)_4^{2-}$. A nitrogen laser was used to excite the crystal.

## Luminescence Studies

**Alkali Halide Environment.** Figure 1 shows the luminescence spectrum at room temperature for a single crystal of NaCl doped with $Pd(CN)_4^{2-}$ ions. The crystal was excited by a nitrogen laser. There are two peaks at 630 nm (15 900 $cm^{-1}$) and at 430 nm (23 300 $cm^{-1}$). The bands are broad and the spectrum extends from 800 to 400 nm. The lifetimes of these peaks have been measured as a function of temperature by studying the decay of emission intensity as a function of time. The higher energy peak was found to have a lifetime less than 10 ns at all temperatures. The lower energy peak has a relatively longer lifetime. At 77 K the lifetime is 700 ns and shows considerable dependence on the temperature. At room temperature the lifetime is of the order of 22 ns. The lifetimes in the range of 77 K to room temperature when plotted as a function of temperature on a semilog graph fall on a straight line as shown in Figure 2. The lifetime measurements have been made for different samples of NaCl doped with $Pd(CN)_4^{2-}$, and the results are consistent.

In order to discuss the luminescence results obtained from mixed crystals of NaCl doped with $Pd(CN)_4^{2-}$ ion, it is necessary to summarize the luminescence results obtained from pure single crystals of $BaPd(CN)_4 \cdot 4H_2O$.[14] In pure single crystals we observed two luminescence maxima, a higher energy band at 382 nm (26 000 $cm^{-1}$) with a width (fwhm) of 900 $cm^{-1}$ and a lower energy band at 512 nm (19 500 $cm^{-1}$) with a width of 3300 $cm^{-1}$. The higher energy peak has a very short lifetime (<10 ns) at all temperatures and was interpreted as fluorescence. The lower energy peak has a longer lifetime which was very much dependent on the temperature. At 77 K the lifetime is about 300 μs. The low-energy peak was interpreted as due to phosphorescence.

The high-energy luminescence peak at 430 nm for $Pd(CN)_4^{2-}$ in NaCl crystals has a very short lifetime and is interpreted as due to fluorescence. This peak is very similar to the high-energy peak observed in pure single crystals of $BaPd(CN)_4 \cdot 4H_2O$ as regards its position and lifetime. A very short lifetime for this peak indicates that the transition is from a singlet excited state. The low-energy peak for the NaCl–$Pd(CN)_4^{2-}$ system at 630 nm is similar to the low-energy peak observed in the emission spectrum of a pure single crystal of $BaPd(CN)_4 \cdot 4H_2O$. This band may be a phosphorescence band. It is very broad as in the case of the pure single crystal. Its lifetime of 700 ns at liquid-nitrogen temperature is much greater than that of the high-energy peak by several hundreds

(3) J. W. Lynn, M. Iizumi, G. Shirane, S. A. Werner, and R. B. Saillant, *Phys. Rev. B: Solid State*, **12**, 1154 (1976).
(4) H. Yersin, *J. Chem. Phys.*, **68**, 4707 (1978).
(5) B. G. Anex and R. L. Musselman, *J. Phys. Chem.*, **84**, 883 (1980).
(6) R. L. Musselman, Ph.D. Thesis, New Mexico State University, 1972.
(7) M. L. Moreau-Colin, *Struct. Bonding (Berlin)*, **10**, 167 (1972).
(8) C. J. Ballhausen, H. Bjerrum, R. Dingle, K. Eriks, and C. R. Hare, *Inorg. Chem.*, **4**, 514 (1965).
(9) C. Moncuit, *J. Chim. Phys.*, **64**, 494 (1967).
(10) S. Yamada, *J. Am. Chem. Soc.*, **73**, 1182 (1951).
(11) S. B. Piepho, P. N. Schatz, and A. J. McCaffery, *J. Chem. Soc.*, **91**, 5994 (1969).
(12) C. D. Cowman and H. B. Gray, *Inorg. Chem.*, **15**, 2823 (1976).
(13) A. Kasi Viswanath, M. B. Krogh-Jespersen, J. Vetuskey, C. Baker, W. D. Ellenson, and H. H. Patterson, *Mol. Phys.*, **42**, 1431 (1981).
(14) W. D. Ellenson, A. Kasi Viswanath, and Howard H. Patterson, *Inorg. Chem.*, **20**, 780 (1981).

**Table I.** Luminescence Results for $Pd(CN)_4^{2-}$ in Different Environments

| system | λ,[b] nm | $E$,[c] $cm^{-1}$ | $\tau$,[d] ns ($T$, K) |
|---|---|---|---|
| $Pd(CN)_4^{-2}$-NaCl | 630 | 15 900 | 700 (77) |
| | | | 22 (300) |
| | 430 | 23 300 | <10[e] |
| $BaPd(CN)_4 \cdot 4H_2O$ | 512 | 19 500 | $\sim 3 \times 10^5$ (77) |
| | 382 | 26 000 | <10[e] |
| $Pd(CN)_4^{-2}$-NaCN | 510 | 19 600 | <20[e] |
| $Pd(CN)_4^{-2}$-KCN[a] | 530 | 18 900 | <10[e] |
| | 370 | 27 000 | <10[e] |

[a] In another sample we observed two peaks at 585 nm (17 100 $cm^{-1}$) and 370 nm (27 000 $cm^{-1}$), both having a lifetime <10 ns. [b] Luminescence wavelength. [c] Luminescence energy. [d] Lifetimes. [e] Room-temperature and 77 K values.

of magnitude. Such a long lifetime indicates that the transition is from a triplet excited state. The peak positions of these two bands are shifted to lower energies in the NaCl crystal as compared to the energy levels in the pure crystal. However, the singlet–triplet separations are of the same order of magnitude in doped and pure crystals. The singlet–triplet separation in the pure crystal is approximately $7 \times 10^3$ $cm^{-1}$ while the same separation in the NaCl crystal is $8 \times 10^3$ $cm^{-1}$.

It is interesting to compare the single–triplet separation in the palladium compound with the analogous platinum salts. Yersin et al.[15] have studied the emission spectra of a series of tetracyanoplatinate compounds with varying metal–metal distance and observed emission from both the lowest energy singlet and triplet excited states. The maximum separation of the singlet–triplet energy levels observed is only $3 \times 10^3$ $cm^{-1}$ This can be understood by considering the fact that the platinum spin–orbit coupling is much greater than palladium.

In our studies of $Pt(CN)_4^{2-}$-doped NaCl crystals, we observed the presence of different types of clusters by site-selective laser spectroscopy.[13] In the present studies, also, we did the selective excitations in the range 260–337 nm by using a tunable dye laser. We did not observe any changes in the luminescence spectrum, and hence it suggests that we have only one type of cluster in the NaCl lattice.

It is possible that the two luminescence peaks for $Pd(CN)_4^{2-}$ doped in NaCl correspond to two different sites where each site is characterized by a particular defect configuration. We have ruled out this possibility because the lifetimes of the two peaks are drastically different, one with a short lifetime and the other with a longer lifetime several times greater than the short one. Thus, it is reasonable to argue that the two peaks are from a single unit, one from a singlet state and the other from a triplet state. All the luminescence results obtained in the present studies are summarized in Table I.

In the case of KCl crystals doped with $Pd(CN)_4^{2-}$ ions, the luminescence is very weak and a good spectrum could not be recorded. This indicates that the palladium cluster species concentration is very small in the KCl host.

**Alkali Cyanide Environment.** Figure 3a shows the luminescence spectrum of an NaCN crystal[17] doped with $Pd(CN)_4^{2-}$ ions, recorded at 77 K. At 77 K we observed one band at 510 nm, which is very broad and extends from 700 to 350 nm. Time-resolved experiments strongly suggest that this broad band corresponds to only one electronic transition. It has a very short lifetime of the order of <20 ns. We observed luminescence even at room temperature with the peak position

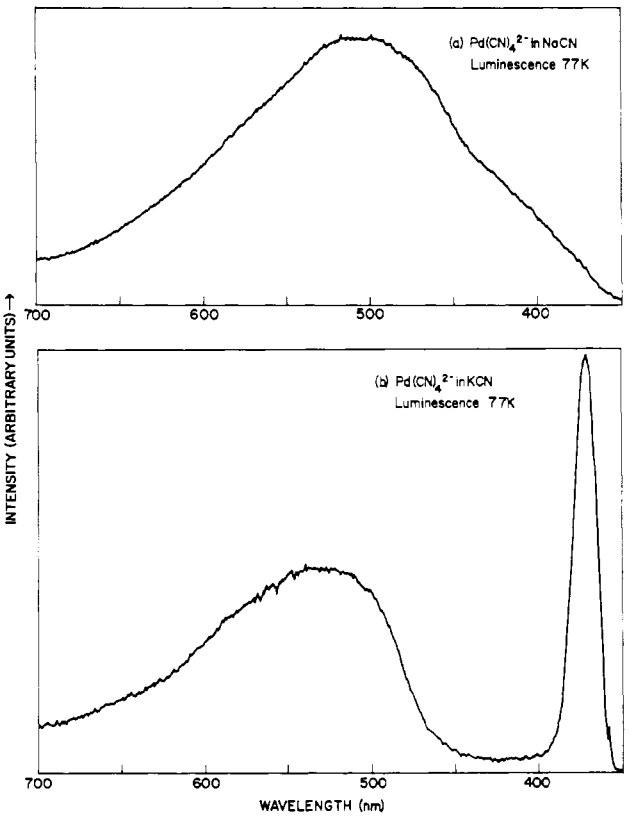


**Figure 3.** (a) Luminescence spectrum of a NaCN crystal doped with $Pd(CN)_4^{2-}$ ions, recorded at 77 K. (b) Luminescence spectrum of a KCN crystal doped with $Pd(CN)_4^{2-}$ ions, recorded at 77 K. A nitrogen laser was used as the excitation source in both the cases.

at 490 nm. Such a short lifetime indicates that the transition is from a singlet excited state. We interpret this peak as due to fluorescence from a cluster. The absorption spectrum of an NaCN crystal doped with $Pd(CN)_4^{2-}$ has peaks at energies less than 250 nm. Fluorescence so far from this absorption indicates that non-monomer cluster species present in small concentration must be responsible for this emission.

Figure 3b shows the 77 K luminescence spectrum of a KCN crystal doped with $Pd(CN)_4^{2-}$ ions. There are two peaks at 370 and 530 nm. The 370-nm peak is quite narrow with a short lifetime of the order of <10 ns, indicating that the emission is from a singlet excited state. This we interpret as due to a cluster. The 530-nm peak is quite broad and is very asymmetric, with a short lifetime ($\tau$ <10 ns). There may be two peaks under this peak, but we could not resolve them even by time-resolved experiments. We interpret this peak also as due to a cluster of $Pd(CN)_4^{2-}$ ions. In another sample of KCN, we observed peaks at 370 and 585 nm. This peak at 370 nm is unchanged in position with change of sample. The peak at 580 nm is due to another cluster of $Pd(CN)_4^{2-}$ ions. We conclude that KCN crystals have different kinds of cluster sites in the lattice. This is also supported by the absorption data that is presented in a later part of this paper. In our earlier studies of KCN doped with $Pt(CN)_4^{2-}$ ions, also, we observed the presence of such cluster impurities in the lattice.[13]

### Absorption Results

**Alkali Halide Environment.** The absorption spectrum of $Pd(CN)_4^{2-}$ doped in KCl at room temperature shows a peak shoulder at about 270 nm (37 000 $cm^{-1}$), a broad absorption band at 231 nm, and a shoulder at 225 nm. A high-energy band occurs at about 190 nm with some indication of structure.

At a mixed-crystal temperture of 78 K or colder, the 270-nm shoulder (see Figure 4) becomes a definite peak at 270 nm with distinct adjacent peaks at 285 (35 100 $cm^{-1}$) and 250 nm

(15) H. Yersin, G. Gliemann, and U. Rössler, *Solid State Commun.*, **21**, 915 (1977).
(16) A. Kasi Viswanath and Max T. Rogers, to be submitted for publication.
(17) Both NaCN and KCN have the *Fm3m* NaCl crystal structure at room temperature, but at 283 and 167 K they exhibit phase transitions. The details are discussed by A. F. Wells, "Structural Inorganic Chemistry", 3rd ed., University Press, Oxford, England, 1962.

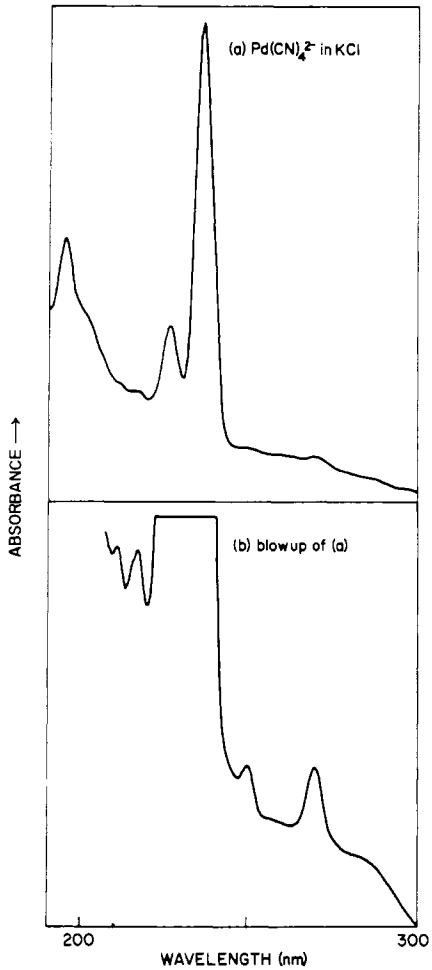


**Figure 4.** (a) Absorption spectrum of a KCl crystal doped with $Pd(CN)_4^{2-}$ recorded at 77 K. (b) Blowup of (a) at 77 K.

(40 000 $cm^{-1}$) now appearing. Also the 225-nm shoulder becomes a definite medium peak at 224 nm and a weak peak at 217 nm. Finally, the 190-nm band shows structure at 212 (w), 202 (m), and 194 nm (s).

Magnetic circular dichroism experiments on various $Pd(CN)_4^{2-}$–KCl crystals at room temperature show a large MCD A term for the 237-nm peak and a weak MCD A term for the 270-nm peak. Unfortunately, we were unable to record the MCD spectra for wavelengths less than 215 nm. From the MCD spectra we must assign the 237- and 270-nm peaks to transitions in which the excited states have electronic degeneracy.

When $Pd(CN)_4^{2-}$ is doped into a KCl lattice, it is known[17] that $Pd^{2+}$ substitutionally replaces a $K^+$ ion and four cyanide ligands replace four $Cl^-$ ions. Charge conservation can be achieved by the absence of a cation in the nearest-neighbor position ($z$ defect) or in a nearest-neighbor position ($xy$ defect). For $Pd(CN)_4^{2-}$ in NaCl or KCl, ESR studies by Viswanath and Rogers[17] show that $Pd(CN)_4^{2-}$ exists in these lattices as a monomer with $C_{4v}$ site symmetry. The palladium cluster species observed in the luminescence experiments are not detected with ESR or optical absorption experiments because of their low concentrations.

In an effort to compare the electronic transitions for $Pd(CN)_4^{2-}$ as an isolated monomer vs. $Pd(CN)_4^{2-}$ as an impurity ion in an alkali halide lattice with a $C_{4v}$ defect, we have carried out extended Hückel MO calculations.[18] The valence electrons have been described by single Slater-type orbitals and

(18) See R. Hoffman, *J. Chem. Phys.*, **39**, 1397 (1963).

**Table II.** Parameters[a] for Extended Hückel Molecular Orbital Calculations

| orbital | $H_{ii}$, eV | exponent |
|---|---|---|
| C 2s | −21.43 | 1.55 |
| C 2p | −11.42 | 1.325 |
| Cl 3s | −24.00 | 2.245 |
| Cl 3p | −15.10 | 1.85 |
| K 4s | −8.6 | 0.595 |
| N 2s | −27.50 | 1.875 |
| N 2p | −14.49 | 1.65 |
| Na 3s | −5.10 | 0.90 |
| Na 3p | −3.00 | 0.533 |
| Pd 5s | −8.99 | 2.24 |
| Pd 5p | −4.41 | 2.09 |
| Pd 4d | −11.16 | 2.852 |

[a] Cl parameters from F. A. Cotton and C. B. Harris, *Inorg. Chem.*, 6, 369 (1967); Na, C, and N parameters from G. Burns, *J. Chem. Phys.*, 41, 1521 (1964); K parameters from K. B. Hathaway and A. Krumhansi, *ibid.*, 63, 4313 (1975); Pd parameters from J. Harrison, Master's Thesis, University of Maine, 1975.

valence orbital ionization potentials have been taken from the literature. The parameters are listed in Table II. In order to model the effect of placing a $Pd(CN)_4^{2-}$ ion in an alkali halide lattice with the defect such that the Pd ion has $C_{4v}$ symmetry,[19] we have proceeded as follows. $C_{4v}$ symmetry has been simulated by placing an anion above and below the $Pd(CN)_4^{2-}$ anion on the $z$ axis as in an alkali halide. Further a cation is placed as in the alkai halide lattice in the $+z$ but not in the $-z$ axis to give the $Pd(CN)_4^{2-}$ ion $C_{4v}$ site symmetry.

The MO calculations predict that for both the isolated monomer and the $C_{4v}$ alkali halide defect cases for $Pd(CN)_4^{2-}$ the MO relative orbital energies are in the order $d_{xy} < d_{xz}$, $d_{yz} < d_{z^2} < a_{2u} < e_u$. For $Pd^{2+}$ the $d_{xy}$, $d_{xz}$, $d_{yz}$, and $d_{z^2}$ orbitals are occupied, and, thus, $Pd(CN)_4^{2-}$ has a $^1A_{1g}$ ground electronic state. The $a_{2u}(\pi^*)$ molecular orbital is a linear combination of the $6p_z$ Pt orbital and the four $\pi^*$ ligand orbitals lying perpendicular to the molecular plane.[20] The $e_u(\pi^*)$ MO is a combination of the Pt $6p_x$, $6p_y$ orbitals and ligand $\pi^*$ orbitals in the molecular plane.[20] The MO calculations indicate that the $d_{x^2-y^2}$ orbital is at higher energies than the $e_u$ orbital, and, thus, transitions to this orbital will be in the far-UV region and not be observed. The $d \rightarrow a_{2u}$ transitions are

$$d_{xy} \rightarrow a_{2u}\ (^1A_{1g} \rightarrow {}^2B_{1u}, {}^3B_{1u})$$
$$d_{xz}, d_{yz} \rightarrow a_{2u}\ (^1A_{1g} \rightarrow {}^1E_u, {}^3E_u)$$
$$d_{z^2} \rightarrow a_{2u}\ (^1A_{1g} \rightarrow {}^1A_{2u}, {}^3A_{2u})$$

Spin–orbit interaction for palladium(+2) should give rise to some mixing of single and triplet states.[11]

Our molecular orbital calculations for $Pd(CN)_4^{2-}$ indicate that the separation between the $a_{2u}$ and $e_u$ orbitals should be about 2200 $cm^{-1}$ for the isolated monomer and about 4600 $cm^{-1}$ for the $C_{4v}$ KCl defect environment. Thus, the solution absorption spectrum for $Pd(CN)_4^{2-}$ should consist of both $d \rightarrow a_{2u}$ and $d \rightarrow e_u$ transitions in the same energy region; in contrast, the absorption spectrum of a $Pd(CN)_4^{2-}$–KCl crystal should have $d \rightarrow a_{2u}$ transitions at lower energy followed by the $d \rightarrow e_u$ transitions. On this basis we assign the 270- and 237-nm peaks for $Pd(CN)_4^{2-}$–KCl to the $^1A_{1g} \rightarrow {}^3E_u$ ($d_{xz}$, $d_{yz} \rightarrow a_{2u}$) and $^1A_{1g} \rightarrow {}^1E_u$ ($d_{xz}$, $d_{yz} \rightarrow a_{2u}$) transitions, respectively. Also, in the 215-nm energy region we assign the observed absorption peaks to $d \rightarrow e_u$ transitions. Our absorption data

(19) S. C. Jain, A. V. R. Warrier, and M. Abha, *J. Chem. Phys.*, **64**, 3804 (1976).
(20) F. A. Cotton, "Chemical Applications of Group Theory", Interscience, New York, 1963, Chapter 8.

Table III. Absorption Results and Assignments for $Pd(CN)_4^{2-}$ in KCl

| λ, nm | $E$, $cm^{-1}$ | intens | assignt[c] |
|---|---|---|---|
| 285 | 35 100 | w | $E_u(^3A_{2u})$[a] |
| 270 | 37 000 | m | $E_u(^3E_u)$[a] |
| 250 | 40 000 | w | $E_u(^3B_{1u})$[a] |
| 236 | 42 400 | s | $E_u(^1E_{1u})$, $A_{2u}(^1A_{2u})$[a] |
| 226 | 44 200 | m | $E_u(^1B_{1u})$[a] |
| 217 | 46 100 | w | $E_u(^3E_u)$[b] |
| 212 | 47 200 | w | $E_u(^1E_{1u})$, $A_{2u}(^1A_{2u})$[b] |
| 202 | 49 500 | m | $E_u(^1E_u)$, $A_{2u}(^1A_{2u}) + \nu(CN)$[b] |
| 194 | 51 500 | s | $E_u(^1E_u)$, $A_{2u}(^1A_{2u}) + 2\nu(CN)$[b] |

[a] Transitions involving $d \rightarrow a_{2u}$ configuration changes. Assignments based on our MCD results and previous $Ni(CN)_4^{2-}$ and $Pt(CN)_4^{2-}$ assignments.[11] [b] Transitions involving $d \rightarrow e_u$ configuration changes. $\nu(CN)$ progression assigned because of relative peak intensities and spacings. [c] The electronic transitions are from an initial $A_{1g}(^1A_{1g})$ electronic state to the listed final electronic states. The label $E_u(^3A_{2u})$ indicates an $E_u$ electronic state in the presence of spin–orbit interaction which is mostly composed of the $^3A_{2u}$ crystal field state. The interested reader should see ref 11 for a detailed discussion of spin–orbit effects for $Pd(CN)_4^{2-}$ type ions.

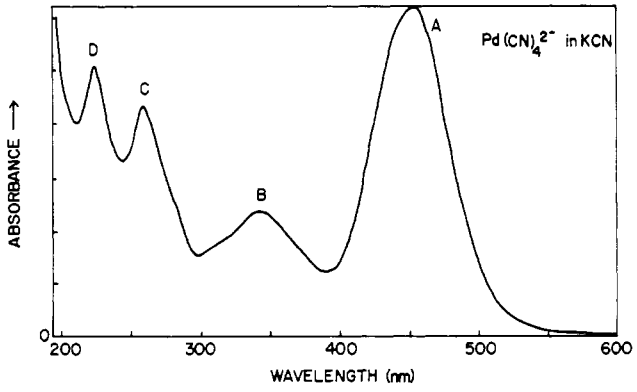


**Figure 5.** Ultraviolet–visible absorption spectrum at room temperature for a KCN crystal doped with $Pd(CN)_4^{2-}$ ions.

and electronic assignments for $Pd(CN)_4^{2-}$–KCl are summarized in Table III.

**Alkali Cyanide Environment.** The UV–visible absorption spectrum at room temperature of a KCN crystal doped with $K_2Pd(CN)_4$ is shown in Figure 5. The lowest energy band (A) is an intense, symmetrical peak at 447 nm (22 400 $cm^{-1}$). The next band (B) occurs at 339 nm (29 500 $cm^{-1}$). The higher energy portion of the spectrum consists of two bands (C and D, respectively) at 258 (38 800 $cm^{-1}$) and 224 nm (44 600 $cm^{-1}$). Our luminescence measurements indicate emission from both bands A and B with lifetimes <20 ns. This implies that the A and B bands correspond to the spin-allowed transitions. Comparison of the $^1A_{2u}$–$^1E_1$ separation in $BaPd(CN)_4$ (17 000 $cm^{-1}$) shows that the same approximate spacing occurs in the KCN environment for the A and C peaks (separation in energy $16.4 \times 10^3$ $cm^{-1}$). This suggests that peaks A and C should be assigned, respectively, to the $^1A_{1g} \rightarrow {}^1A_{2u}$ and $^1A_{1g} \rightarrow {}^1E_u$ transitions. The 38 800-$cm^{-1}$ $^1A_{1g} \rightarrow {}^1E_u$ transition in KCN should be compared with the energy of 42 400 $cm^{-1}$ for this transition in KCl where cluster species are present in low concentrations.

We believe the lowest energy absorption in the KCN environment is some 9000 $cm^{-1}$ lower in energy than the strong low-energy band in $BaPd(CN)_4$ because of the defects in the KCN case. For example, if a $Pd_2$ entity is substituted for two $K^+$ ions, two vacancies at $K^+$ sites will occur and these defects will have an electrostatic effect on the orbitals of the palladium species. Alternatively, if a $Pd_2$ dimer is substituted for $K^+$–$CN^-$–$K^+$, three $K^+$ ions will be absent from the doped crystal

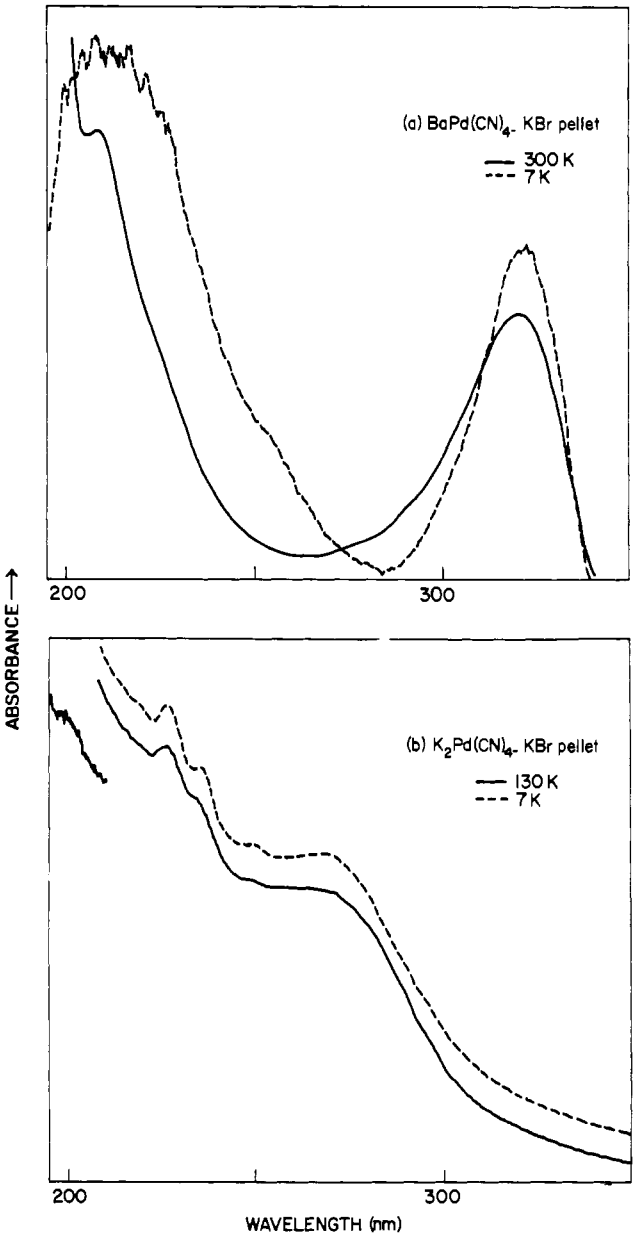


**Figure 6.** (a) Absorption spectra of $BaPd(CN)_4$–KBr pellet at different temperatures. (b) Absorption spectra of $K_2Pd(CN)_4$–KBr pellet at different temperatures.

and again these defects will exert an electrostatic effect on the impurity ion orbital energies. To understand the role of defects, we have done MO calculations for a $Pt(CN)_4^{2-}$ dimer with $xy$ or $z$ defects.[13]

The $Pd(CN)_4^{2-}$–NaCN absorption spectra exhibit maxima at 255, 220, and 197 nm. No appreciable absorption occurs at less than 260 nm. The 225-nm transition is assigned as in KCN to $^1A_{1g} \rightarrow {}^1E_u$. The 220- and 197-nm transitions must arise from $d \rightarrow e_u$ type transitions.

**Pellet Environments.** Our $BaPd(CN)_4$–KBr experimental pellet data are in agreement with the $BaPd(CN)\cdot 4H_2O$ single-crystal-reflectance results of Musselman.[6] This indicates that the pellets are analogous to the single crystals and that metal–metal interactions are present in KBr pellets. In Table IV we have summarized our pellet data for $BaPd(CN)_4$ and $K_2Pd(CN)_4$.

In the room-temperature pellet spectra of $BaPd(CN)_4$ (Figure 6a) there is a symmetrical intense band at 318 nm (31 450 $cm^{-1}$) and a much weaker band at 207 nm (48 300 $cm^{-1}$). As the pellet is cooled to liquid-helium temperature,

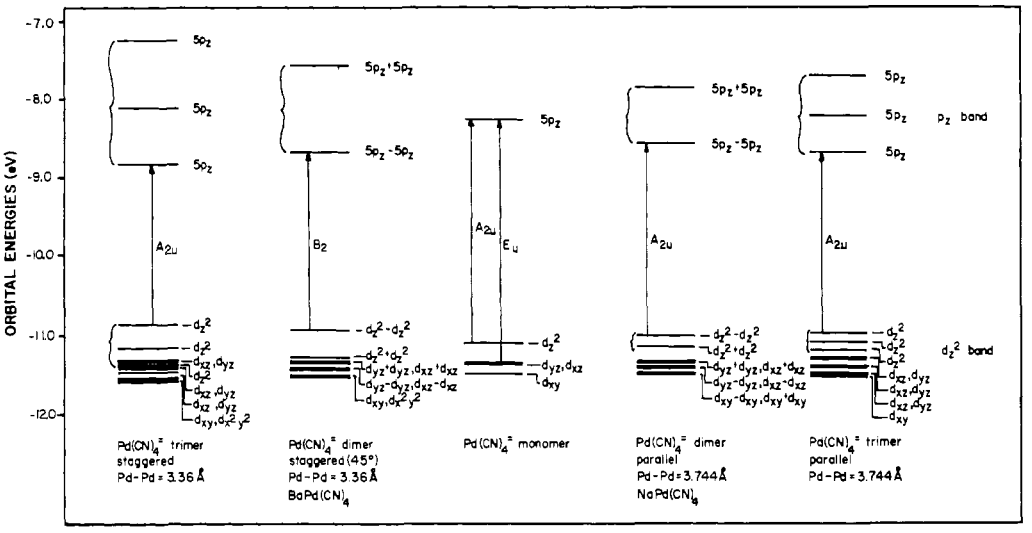


**Figure 7.** Extended Hückel MO results for a monomer, dimer, and trimer of $Pd(CN)_4^{2-}$ ions.

Table IV. Absorption Results and Assignments for KBr Pellets of $BaPd(CN)_4$ and $K_2Pd(CN)_4$

| λ, nm | $E$, $cm^{-1}$ | intens | assignt[b] |
|---|---|---|---|
| | (a) $BaPd(CN)_4$ Case | | |
| 318 | 31 400 ($z$) | s | $A_{2u}(^1A_{2u})$ |
| 207 | 48 300 ($xy$) | s | $E_u(^1E_u)$ |
| | (b) $K_2Pd(CN)_4$ Case | | |
| 270 | 37 000 | s | $A_{2u}(^1A_{2u})$ |
| 250 | 40 000 | w | |
| 235.8 | 42 400 | m | $E_u(^3E_u)$ |
| 225 | 44 400 | s | $E_u(^1E_u)$ |
| 200 | 50 000 | s | $E_u(^1E_u)$[a] |

[a] Transition involving $d \rightarrow e_u$ configuration change. [b] The electronic transitions are from an initial $A_{1g}(^1A_{1g})$ electronic state to the following final electronic states. The irreducible representation before the parenthesis is the resulting state when spin-orbit interaction is nonzero.

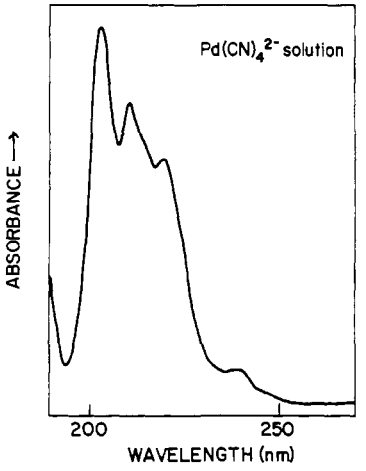


**Figure 8.** Absorption spectrum of $Pd(CN)_4^{2-}$ in aqueous solution at room temperature.

the lowest energy band has the same shape, but the 207-nm band now appears like a real peak instead of just a shoulder and covers the region from 195 to 240 nm. The 318-nm (31 450-$cm^{-1}$) band is $z$ polarized from the Musselman reflectance measurements[6] and so is assigned as $^1A_{1g} \rightarrow {}^1A_{2u}$ ($d_{z^2} \rightarrow a_{2u}$). The $K_2Pd(CN)_4$–KBr pellet results at 7 K show peaks at 270, 250, 235.8, and 225 nm.

In order to model a chain of $Pd(CN)_4^{2-}$ ions, we have carried out monomer, dimer, and trimer MO calculations. The trimer results should approximate the spread of the bands as in a $Pd(CN)_4^{2-}$ polymer chain. The results are shown in Figure 7. From our MO results we predict that in the pellet (polymer case), in comparison to the monomer case, the $d_{z^2} \rightarrow a_{2u}$ transition should be at much lower energy and the $d_{xz}$, $d_{yz} \rightarrow a_{2u}$ transition should be at slightly less energy. Our assignments are summarized in Table IV for $BaPd(CN)_4$ and $K_2Pd(CN)_4$.

**Solution Environment Results.** The solution absorption spectrum (Figure 8) of the $4d^8$ $Pd(CN)_4^{2-}$ ion shows overlapping bands in the 200–250-nm region. The lowest energy band occurs at about 238 nm (42 000 $cm^{-1}$). The band at 220 nm (45 500 $cm^{-1}$) appears only as a shoulder. The remaining two bands are at 211 (47 400 $cm^{-1}$) and 202 nm (49 500 $cm^{-1}$).

In order to assign the $Pd(CN)_4^{2-}$ solution absorption spectra, we will make use of our extended Hückel MO calculations for an isolated $Pd(CN)_4^{2-}$ ion.[18] These calculations indicate that the energy separation of the $a_{2u}$ and $e_u$ orbitals is only about 2500 $cm^{-1}$. Thus, the observed $Pd(CN)_4^{2-}$ solution absorption spectrum should be composed of both $d \rightarrow a_{2u}$ and $d \rightarrow e_u$ transitions occurring at about the same energies. The $d \rightarrow e_u$ transitions are

$$d_{z^2} \rightarrow e_u\ (^1A_{1g} \rightarrow {}^1E_u, {}^3E_u)$$
$$d_{xz}, d_{yz} \rightarrow e_u\ (^1A_{1g} \rightarrow {}^{1,3}A_{1u}, {}^{1,3}A_{2u}, {}^{1,3}B_{1u}, {}^{1,3}B_{2u})$$
$$d_{xy} \rightarrow e_u\ (^1A_{1g} \rightarrow {}^1B_{1u}, {}^3B_{1u})$$

MCD studies of the $Pd(CN)_4^{2-}$ ion in solution by Schatz and co-workers[11] showed no distinct A terms. However, the rather clear dips in the MCD spectrum at about 42 000 and 45 500 $cm^{-1}$,[11] which are not mirrored in absorption, are suggestive of the presence of substantial A terms among the overlapping bands. In contrast, both the $3d^8$ $Ni(CN)_4^{2-}$ and $5d^8$ $Pt(CN)_4^{2-}$ solution MCD spectra[11] show three A terms due to $d \rightarrow a_{2u}$ type transitions. In these two cases there is no evidence of a $d \rightarrow e_u$ transition except for $Ni(CN)_4^{2-}$ at $50.3 \times 10^3$ $cm^{-1}$ where there is a separation of about $13.0 \times 10^3$ $cm^{-1}$ between this transition and the highest energy $d \rightarrow a_{2u}$ observed transition.

If we assign the solution peak at 45 500 $cm^{-1}$ as $d \rightarrow a_{2u}$ ($^1A_{1g} \rightarrow {}^1E_u$) we expect from our MO calculations to find the $d \rightarrow e_u$ ($^1A_{1g} \rightarrow {}^1E_u$) transition in the 48 000-$cm^{-1}$ region. If we assume the spacings for the $d \rightarrow a_{2u}$ and $d \rightarrow e_u$ type transitions in solution are the same as for $Pd(CN)_4^{2-}$–KCl mixed crystals, except for a shift in energy between the two types of transitions, we can assign the $Pd(CN)_4^{2-}$ solution spectrum. The $d \rightarrow a_{2u}$ transitions are predicted to appear at about 38 100, 39 800, 42 800, and 45 200 $cm^{-1}$. The $d \rightarrow$

Table V. Absorption Results and Proposed Assignments for the Solution Spectra of the $Pd(CN)_4^{-2}$ Ion

| exptl $E$, $cm^{-1}$ | calcd $E$, $cm^{-1}$ | assignt |
|---|---|---|
| 40 000[a] | 38 100 | $d \rightarrow a_{2u}$ ($^1A_{1g} \rightarrow {}^3A_{2u}$) |
| | 39 800 | ($^1A_{1g} \rightarrow {}^3E_u$) |
| 43 000[b] | 42 800 | ($^1A_{1g} \rightarrow {}^3B_{1u}$) |
| 45 500[a] | 45 200 | ($^1A_{1g} \rightarrow {}^1E_u, {}^1A_{2u}$) |
| 42 000[a] | 42 000 | $d \rightarrow e_u$ ($^1A_{1g} \rightarrow {}^3E_u$) |
| 43 000[b] | 43 100 | ($^1A_{1g} \rightarrow {}^3A_{1u}, {}^3A_{2u}, {}^3B_{1u}, {}^3B_{2u}$) |
| 45 500[a] | 45 400 | ($^1A_{1g} \rightarrow {}^3B_{1u}$) |
| 47 500[a] | 47 400 | ($^1A_{1g} \rightarrow {}^1E_u, {}^1A_{2u}$) |
| 49 500[a] | | $d \rightarrow b_{1u}$ ($^1A_{1g} \rightarrow {}^1E_u, {}^1A_{2u}$) |

[a] These experimental energies are from Figure 8 of this paper. [b] Schatz et al. reported shoulders in their absorption spectra at 43 000 and 46 500 $cm^{-1}$, and this is the basis of the 43 000-$cm^{-1}$ peak.

$e_u$ transitions should occur at about 42 000, 43 100, 45 400, and 47 400 $cm^{-1}$. The Figure 2 $Pd(CN)_4^{2-}$ solution spectrum of Schatz et al.[11] shows absorption maxima at 42 000, 45 500, and 47 500 $cm^{-1}$ with shoulders at 43 000 and 46 500 $cm^{-1}$. At about 40 000 $cm^{-1}$, the lowest energy observed absorption occurs. We conclude there is reasonable agreement between the experimental solution absorption data of Schatz et al. and the absorption patterns for $Pd(CN)_4^{2-}$ in KCl for the $d \rightarrow a_{2u}$ and $d \rightarrow e_u$ type transitions.

A summary of the absorption results and assignments for $Pd(CN)_4^{2-}$ in solution is given in Table V.


## Summary

We have measured the luminescence and absorption spectra of tetracyanopalladate(II) ions doped into NaCl, KCl, NaCN, and KCN crystals and find evidence for the presence of both monomer and cluster species of $Pd(CN)_4^{2-}$. The luminescence spectra of the palladium-doped alkali halide and alkali cyanide crystals have lifetimes and energies very similar to the luminescence we have reported for pure $BaPd(CN)_4$ crystals; thus, we conclude palladium cluster species are responsible for the luminescence.

The absorption spectra of $Pd(CN)_4^{2-}$ in KCl are assigned on the basis of EPR measurements by Viswanath and Rogers[16] to a $Pd(CN)_4^{2-}$ monomer ion in $C_{4v}$ site symmetry. Simple extended Hückel molecular orbital calculations for such a defect structure suggest that $d \rightarrow a_{2u}$ and $d \rightarrow e_u$ type transitions are separated in energy unlike in solution where they occur at the same energies. In contrast, KCN-doped palladium crystals have a yellow color and have a large percentage of cluster species unlike in KCl where the concentration is very small.


**Acknowledgment.** This research was supported by NSF, Department of Materials Research (Grant DMR 77-07140).

**Registry No.** $Pd(CN)_4^{2-}$, 15004-87-2; NaCl, 7647-14-5; NaCN, 143-33-9; KCN, 151-50-8; KCl, 7447-40-7; $BaPd(CN)_4$, 14038-83-6; $K_2Pd(CN)_4$, 14516-46-2; KBr, 7758-02-3.

Contribution from the Department of Chemistry, University of California at San Diego, La Jolla, California 92093

# Stereochemistry of the Photoaquation of Optically Active Tris(ethylenediamine)chromium(III) as a Probe of Excited-State Pathway

MARC C. CIMOLINO and R. G. LINCK*

*Received September 26, 1980*

The photoaquation of $\Lambda$-$Cr(en)_3^{3+}$ in acidic aqueous solution under ligand field excitation produces three isomers of $Cr(en)_2(enH)(H_2O)^{4+}$, the $\Lambda$-cis, $\Delta$-cis, and trans isomers. Their quantum yields are 0.10, 0.03, and 0.24, independent of wavelength of irradiation from 365 to 685 nm. These data strongly imply reactivity only from the lowest lying quartet state with back intersystem crossing from the lowest doublet state to that quartet accounting for delayed reaction. The results are also analyzed in terms of a model predicting the stereochemical result of photoaquation of Cr(III) complexes.

## Introduction

In this, the third decade of investigation of chromium(III)–amine photochemistry,[1,2] there lurks a question that was asked before:[3-5] Does reactivity occur from the lowest excited state, a doublet state, $^2X$, and/or from the lowest excited quartet state, $^4Y$?[6] In fact, this question was predominant in several studies published in the late 1950s. Plane and co-workers[3,7] and Schläfer argued the long-lived $^2X$ state could account for all photoreactivity because a plausible model for associative attack on this excited $t_{2g}^3$ species could be formulated[9] (and $\phi$ was reported as independent of excitation wavelength). Some years later Adamson[5] suggested that the excited quartet could be reactive, even with a short lifetime. This model became attractive to a number of investigators, has been the basis of several models[10-12] of photoaquation, and is now generally accepted as the conventional wisdom. Especially important experiments establishing that the $^4Y$ state was reactive (even though perhaps not the exclusive reactive state) are those of Chen and Porter[13] and Wasgestian.[14] However, several studies have appeared recently that have been interpreted to implicate partial reactivity from the $^2X$ state. This has been suggested especially in the case of *trans*-Cr-

* To whom correspondence should be addressed at the Department of Chemistry, Smith College, Northampton, MA 01063.


(1) Zinato, E. In "Concepts of Inorganic Chemistry"; Adamson, A. W., Fleischauer, P. D., Eds.; Wiley: New York, 1975; pp 143–201.
(2) Balzani, V.; Carassiti, V. "Photochemistry of Coordination Compounds"; Academic Press: New York, 1970.
(3) Edelson, M. R.; Plane, R. A. *Inorg. Chem.* **1964**, *3*, 231.
(4) Schläfer, H. L. *J. Phys. Chem.* **1965**, *69*, 2201.
(5) Adamson, A. W. *J. Phys. Chem.* **1967**, *71*, 798.
(6) The states are labeled $^4Y$ and $^2X$ to avoid specific comment on the symmetry of states that *must* be Jahn–Teller distorted in their equilibrium geometry.
(7) Plane, R. A.; Hunt, J. P. *J. Am. Chem. Soc.* **1957**, *79*, 3343.
(8) Schläfer, H. L. *Z. Phys. Chem. (Wiesbaden)* **1957**, *11*, 65.
(9) Taube, H. *Chem. Rev.* **1952**, *50*, 69.
(10) Zink, J. I. *J. Am. Chem. Soc.* **1972**, *94*, 8039.
(11) Wrighton, M.; Gray, H. B.; Hammond, G. S. *Mol. Photochem.* **1973**, *5*, 165.
(12) Vanquickenborne, L. G.; Ceulemans, A. *J. Am. Chem. Soc.* **1977**, *99*, 2208.
(13) Chen, S. N.; Porter, G. B. *Chem. Phys. Lett.* **1970**, *6*, 41. See also: Porter, G. B.; Chen, S. N.; Schläfer, H. L.; Gausmann, H. *Theor. Chim. Acta* **1971**, *20*, 81.
(14) Wasgestian, H. F. *J. Phys. Chem.* **1972**, *76*, 1947.


0020-1669/81/1320-3499$01.25/0 